DMD chip space evaluation for ESA's EUCLID mission

Frederic Zamkotsian, Emmanuel Grassi, Patrick Lanzoni, Rudy Barette, Christophe Fabron, et al.

Frederic Zamkotsian, Emmanuel Grassi, Patrick Lanzoni, Rudy Barette, Christophe Fabron, Kyrre Tangen, Laurent Marchand, Ludovic Duvet, "DMD chip space evaluation for ESA's EUCLID mission," Proc. SPIE 7596, Emerging Digital Micromirror Device Based Systems and Applications II, 75960E (18 February 2010); doi: 10.1117/12.845690

SPIE.

Event: SPIE MOEMS-MEMS, 2010, San Francisco, California, United States

DMD chip space evaluation for ESA EUCLID mission

Frederic Zamkotsian[1], Emmanuel Grassi[1], Patrick Lanzoni[1], Rudy Barette[1], Christophe Fabron[1], Kyrre Tangen[2], Laurent Marchand[3], Ludovic Duvet[3]

[1]Laboratoire d'Astrophysique de Marseille, CNRS, 38 rue Frederic Joliot Curie, 13388 Marseille Cedex 13, France
[2]Visitech, Kjellstadveien 5, Lier, P.O.Box 616, N-3003 Drammen, Norway
[3] European Space Agency, Keplerlaan 1, 2200 AG, Noordwijk, The Netherlands

E-mail address: frederic.zamkotsian@oamp.fr

ABSTRACT

The EUCLID mission from the European Space Agency (ESA) will study the dark universe by characterizing a very high number of galaxies in shape and in spectrum. The high precision spectra measurements could be obtained via multi-object spectroscopy (MOS) using Digital Micromirror Devices (DMD). These devices would act as object selection reconfigurable masks. ESA has engaged with Visitech and LAM in a technical assessment of the DMD from Texas Instruments that features a 2048 x 1080 mirrors and a 13.68µm pixel pitch for space applications. For EUCLID, the device should work in vacuum, at low temperature, and each MOS exposure lasts 1500s with micromirrors held in a static state (either ON or OFF) during that duration.
A specific thermal / vacuum test chamber has been developed for test conditions down to -40°C at 10^{-5} mbar vacuum. Imaging capability for resolving each micromirror has also been developed for determining any single mirror failure. Dedicated electronics and software permit to hold any pattern on the device for a duration as long as 1500s. Our first tests reveal that the DMD remains fully operational at -40°C. A 1038 hours life test, in EUCLID conditions (temperature and vacuum) has been successfully completed. Total Ionizing Dose (TID) radiation tests have been completed, establishing between 10 and 15 Krads, the level of TID that the DMD can tolerate; at mission level, this limitation could most likely be overcome by a proper shielding of the device. Finally, thermal cycling, vibration tests and MOS-like tests are under way.

Keywords: micromirror array, technical assessment for space, multi-object spectrograph, EUCLID mission, MOEMS.

1. INTRODUCTION

The EUCLID mission from the European Space Agency (ESA) will study the dark universe by characterizing a very high number of galaxies in shape and in spectrum. In order to optimize the Signal-to-Noise Ratio (SNR) value, the high precision spectra measurements could be obtained via multi-object spectroscopy (MOS). Multi-object spectroscopy (MOS) with multi-slits is the best approach to eliminate the problem of spectral confusion, to optimize the quality and the SNR of the spectra, to reach fainter limiting fluxes and to maximize the scientific return both in cosmology and in legacy science.

Major telescopes around the world are equipped with Multi-Object Spectrographs (MOS) in order to simultaneously record several hundred spectra in a single observation run. Next generation MOS for space like the Near Infrared Multi-Object Spectrograph (NIRSpec) for the James Webb Space Telescope (JWST) require a programmable multi-slit mask. Conventional masks or complex fiber-optics-based mechanisms are not attractive for space. The programmable multi-slit mask requires remote control of the multi-slit configuration in real time.

A promising possible solution is the use of MOEMS devices such as micromirror arrays (MMA) [1,2,3] or micro-shutter arrays (MSA).[4] MMAs are designed for generating reflecting slits, while MSAs generate transmissive slits. MSA has been selected to be the multi-slit device for NIRSpec and is under development at the NASA's Goddard Space Flight Center. They use a combination of magnetic effect for shutter actuation, and electrostatic effect for shutter latching in

Emerging Digital Micromirror Device Based Systems and Applications II, edited by Michael R. Douglass, Larry J. Hornbeck,
Proc. of SPIE Vol. 7596, 75960E · © 2010 SPIE · CCC code: 0277-786X/10/$18 · doi: 10.1117/12.845690

the open position. In Europe, an effort is currently under way to develop single-crystalline silicon micromirror arrays for future generation infrared multi-object spectroscopy.[5]

By placing the programmable slit mask in the focal plane of the telescope, the light from selected objects is directed toward the spectrograph, while the light from other objects and from the sky background is blocked. For example, a MOEMS-based MOS concept where the programmable slit mask is a MMA is shown in the left-hand side of Fig. 1. Using a MMA, any required slit configuration might be obtained with the capability to match point sources or extended objects (Fig. 1). In action, the micro-mirrors in the ON position direct the light toward the spectrograph and appear bright, while the micro-mirrors in the OFF position are dark.

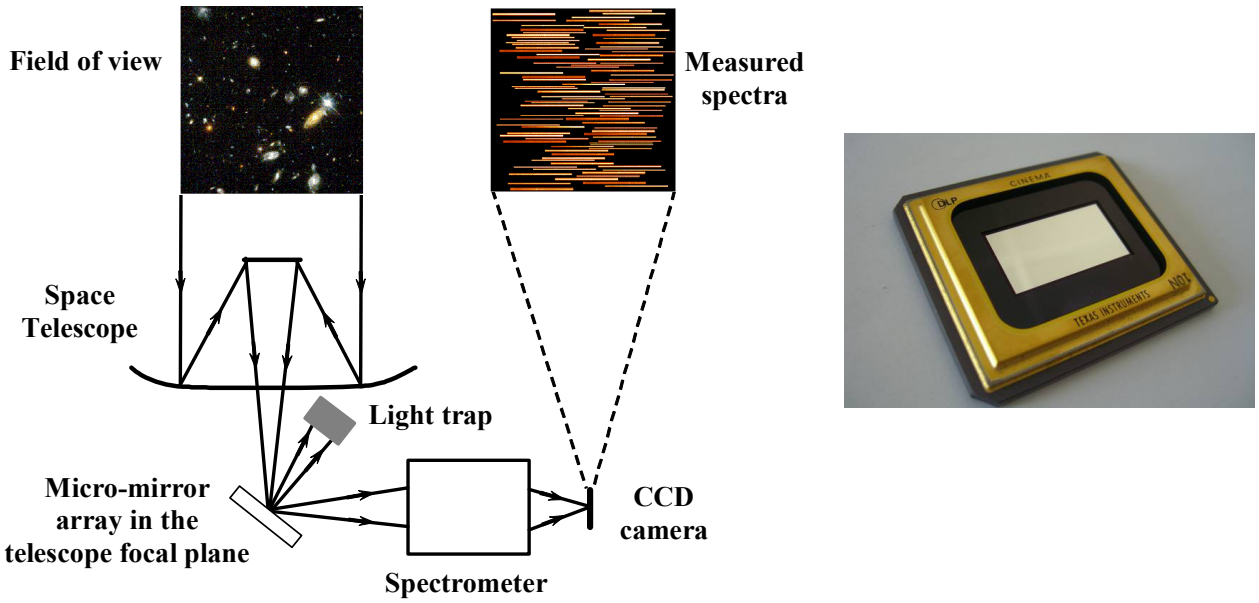

Fig. 1: Principle of a Multi-Object Spectrograph with a Micro-Mirror Array.
DMD chip from Texas Instruments (2048 x 1080 micromirrors).

In the timescale of the EUCLID mission, a specialized programmable multi-slit mask cannot be developed. This component has to be commercially available. To get more than 2 millions independent micromirrors, the selected component for an EUCLID pre-study is a DMD chip from Texas Instruments that features 2048 x 1080 mirrors and a 13.68µm pixel pitch (right-hand side of Fig. 1). Typical operational parameters are room temperature, atmospheric pressure and mirrors switching thousands of times in a second, while for EUCLID, the device should work in vacuum, at low temperature, and each MOS exposure lasts between 400s and 1500s, with mirrors held in one state (either ON or OFF) during the exposure.

In Laboratoire d'Astrophysique de Marseille (LAM), we have developed over several years different tools for the modeling and the characterization of these MOEMS-based slit masks, during the design studies on JWST-NIRSpec. [6,7] ESA has engaged with Visitech and LAM in a technical assessment of a DMD chip for space application. A specific thermal / vacuum test chamber has been developed for test conditions down to -40°C at 10^{-5} mbar vacuum. Imaging capability for resolving each micro-mirror has also been developed for determining any single mirror failure. A dedicated electronics and software permit to hold any pattern on the device for duration as long as 1500s. Tests in vacuum at low temperature, radiations, vibrations, thermal cycling, and preliminary life tests have been scheduled.

We present in this paper, the electronic test vehicle as well as the cold temperature test set-up we have developed. Then, results of radiation tests, tests in vacuum at low temperature, and endurance life test are presented.

2. THE ELECTRONIC TEST VEHICLE

This paragraph provides a description of the electronic test vehicles. The first section describes some of the specific requirements that the test vehicles had to fulfill, the next section explains the details on how the various modes of the DMD were created and the last section deals with a brief description of the main parts of the electronic test vehicles.

2.1 Architecture of the electronic test vehicles

The DMD driver electronics consists of a formatter board and a DMD board. The general architecture of the system is described in Figure 3. There is a notable difference that separates this system from other designs; the control signals of the DAD1000 reset drivers are fed through an FPGA. This enables splitting the DMD into five zones with each zone being driven with a different pattern and refresh rate. This functionality reduces the number of test vehicles and test duration because several conditions can be tested in parallel on the same DMD. An explanation of the functionality can be found in paragraph 2.3. The following is a brief description of the building blocks of the system

Formatter board, RS232 input: The input enables control of the formatter board from a PC during testing.

Formatter board, DVI input: The input receives test images from a PC and transfer them to the FPGA.

Formatter board, FPGA: 1) The integrated micro controller handles RS232 communication and programs the DDP1000 formatters. 2) The signals from the DVI input are processed before being sent to the DDP1000 formatters. 3) Manipulation of the DAD1000 reset drivers control signals, details can be found in paragraph 4.

Formatter board, DDP1000: The two DDP1000 formatters handle DMD image processing. Each formatter has a corresponding RAMBUS memory.

DMD board: The DMD board contains the DMD and two DAD1000 reset drivers.

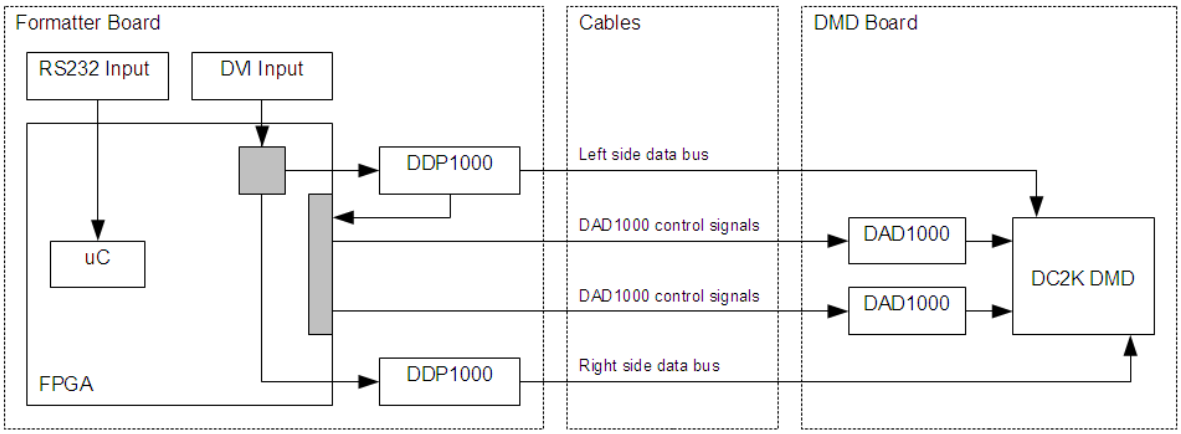

Figure 3: Block diagram of the formatter and DMD board.

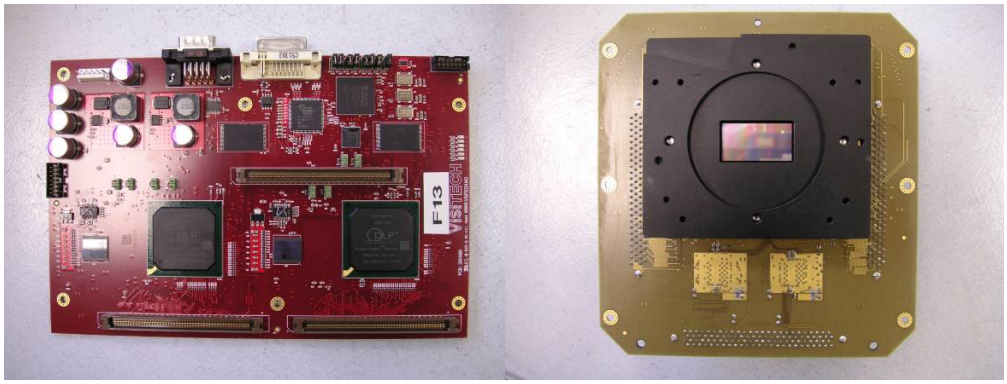

Figure 4: Pictures of the formatter and DMD board.

2.2 Environmental requirements for the electronic test vehicles

The electronic test vehicles were designed by Visitech for extreme test conditions using essentially commercial off the shelf components. In addition, the EUCLID DMD operation requires that each DMD micromirror will be held in one position for 1500 seconds at a time. The budget and schedule of the EULID pre-study meant that compromises had to be made, and the following describes some of the compromises and how we minimized risk and potential impact to the budget and schedule.

Low temperature operation: Except for the DMD, DDP1000, DAD1000 and the RAMBUS memory, the system uses commercial off the shelf components, which can operate at -40°C.

Vacuum operation: The DMD board has no protective coating or printed reference designators that can cause outgassing. All components on the DMD board were selected in an attempt to avoid outgassing materials.

Radiation testing: Careful layout of the components on the electronics boards allowed for efficient shielding of active components that should not be radiation tested. Current sense resistors enabled current measurements during and in between radiation testing.

2.3 DMD zones and modes

In addition to the extreme conditions of a EUCLID environment, this DMD-based instrument also has a very unusual DMD operation: during data capture, each DMD micromirror will be held in one position for 1500 seconds before changing state. This is quite a challenge to accomplish with a DDP1000 based chip set and testing is required in static ON and static OFF modes in addition to normal operation. Normal operation is used as a base line in analyzing test results. Neither the budget nor schedule of the ESA activity allowed testing on separate devices.

To meet all requirements, Visitech constructed a test vehicle that divides each DMD into 5 horizontal zones and each zone can be driven in normal mode or static modes. This test vehicle allows for testing of all modes on a single DMD at the same time. 4/5 of the DMD operates in a static ON or OFF mode (arbitrary pattern) and 1/5 of the DMD operates in display-type mode where the pattern is updated at 1Hz rate. This results in a display-type zone of roughly 400 000 micromirrors and static zones of 4 times this size, which is an ample amount for statistical analysis of the test results. The various zones are created in three stages by decoding and controlling the control signals of the DAD1000 reset drivers with the FPGA

1. A test pattern is written to the DMD and the DAD1000 control signals are in a FPGA pass through mode.
2. The FPGA decodes the DAD1000 control signals and waits for a global reset to occur. A global reset loads the test pattern written to the DMD onto the DMD micromirrors.
3. The FPGA stops the DAD1000 control signals for the static zones and generates a reset sequence for the normal operation zone so that the DMD micromirrors in this zone is updated with new image content.

3. COLD TEMPERATURE TEST EQUIPMENT AND PROCEDURE

The Laboratoire d'Astrophysique de Marseille has over the last few years developed an expertise in the characterization of micro-optical components. [7,8,9] This expertise in small-scale deformation characterization on the surface of micro-optical components as well as operational testing of MOEMS components has been used for developing a dedicated cold temperature test set-up for DMD measurements in EUCLID operating conditions.

3.1Cryostat & optical bench

For environmental testing (vacuum and low temperature), a cryostat has been developed at LAM. The bench (Fig. 5) is used as a photometric bench. In order to get enough resolution on each micromirror, the FOV covers about 200x200 micromirrors on a 1k x 1k camera. For complete DMD testing, a stitching procedure is carried out, by means of motorized stages. For the accuracy and the duration of all these tests, the characterization set-up is automated as much as possible. Three computers are used for managing the tests: the *cryostat computer* for thermal and vacuum environment, the *test computer* for all testing equipment (stages, camera) and the *DMD computer* for driving the DMD.

The thermal chamber enables tests in a vacuum environment with temperature adjustment in the range of -60°C to +20°C. Temperature change are obtained through a liquid cooler. The chamber is made of a stainless steel cross. Each

side is devoted to a specific task. The first side includes a window in order to view the DMD sample; the second side holds the feed-through connectors for driving the DMD board; the third side permits all sensing wires (for temperature sensors) to pass into the chamber. Finally, the fourth side receives the pipes from the liquid cooler device. The cryostat is monitored with temperature sensors and vacuum sensors driven by a computer (*cryostat computer* in Fig. 5). Illumination of the whole array is made by a collimated beam. Optical imaging is made by two doublets (200mm – 400mm) mounted on rail. The system is diffraction limited on the detector, leading to an optimized photometric measurement. The device is divided into **50 zones**. The FOV to be imaged by the CCD camera will cover one zone, equivalent to **205 x 216 micromirrors** (44280 micromirrors). The plate scale on the 1k x 1k camera is exactly 4.07 x 4.07 detector pixels / micromirror. For complete DMD testing, the stitching procedure is done by means of Newport – MicroContrôle motorized stages in three directions (XYZ), with a travelling range of 100mm and a resolution of 0.1µm. The optical test equipment (stages + camera) are monitored by a computer (*test computer* in Fig. 5). All software is developed in Matlab.

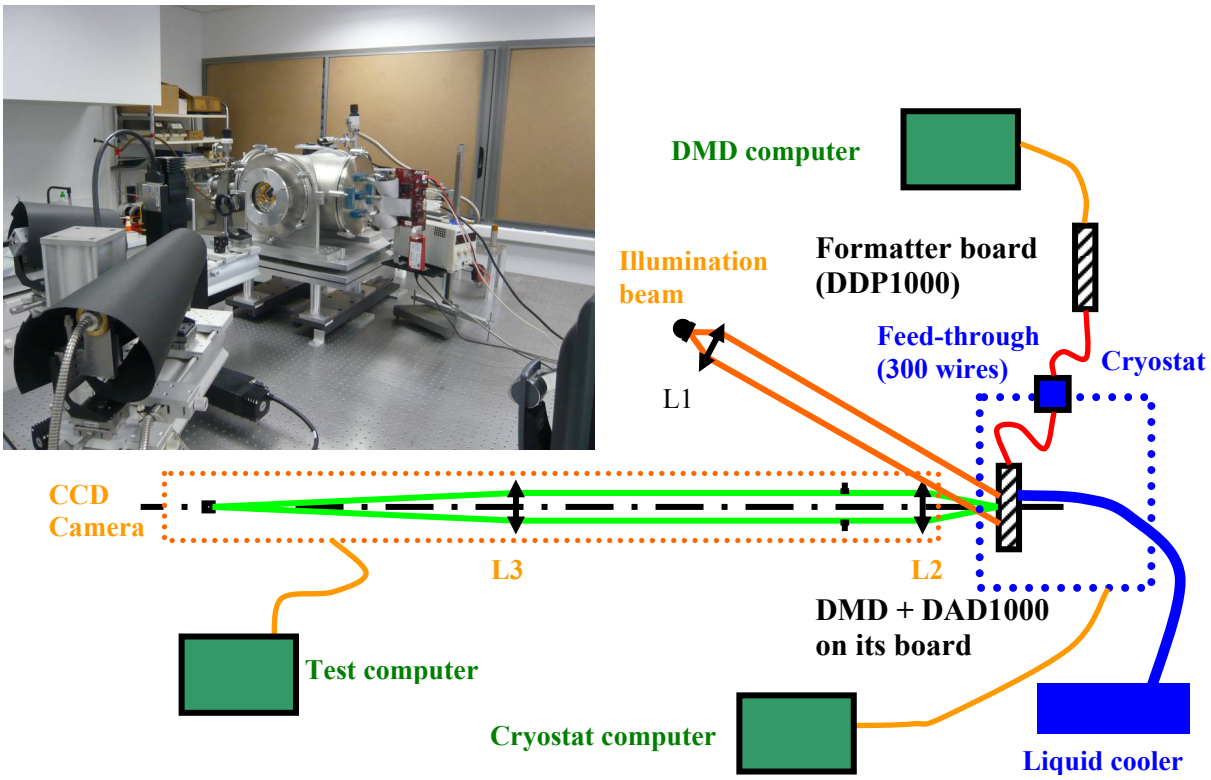

Figure 5: Cold temperature test set-up

3,2 Integration

The DMD board is mounted on the thermal interface through a point-plane-plane mounting in order to avoid any additional stress on the board when the temperature is changing. The thermal link between the thermal interface and the DMD board as well as the DMD itself is done through copper wires connected to the DMD board, the DMD heat sink and the front mounting surface of the DMD device. The DMD board is linked by 300 wires through the chamber to the formatter board. Specialized feed-throughs for such high number of wires have been realized, tested, and have been mounted on our chamber. All materials used in the chamber are vacuum compatible, except the wires leading to the DMD board and some parts on the DMD board, see section 3.1 for details. After DMD board integration, the thermal screen with Multi-Layer Insulator (MLI) cover is mounted around the device, and the optical window is closed on the chamber (Fig. 5). We have decided to align and fix the optical input and output beams as a very precise and reliable reference. Then all optical alignments are performed on the chamber, using the tip-tilt and rotation mounting under the cryo chamber. When the DMD chip and the detector are in parallel planes, the stitching of the images could be done much easier with the motorized stages moving the optical train. A focused image along the whole device is maintained

without using the Z stage during stitching with the X and Y stages. By this way, the optical input and output beams stay fixed.

3.3 Device driving

Hardware and software were developed by Visitech and LAM for driving the DMD boards. The hardware is controlled by a RS-232 serial link and a DVI port is used for image loading on the DMD. The software is developed in Matlab for driving the DMD chip, by a computer (*DMD computer* in Fig. 5).

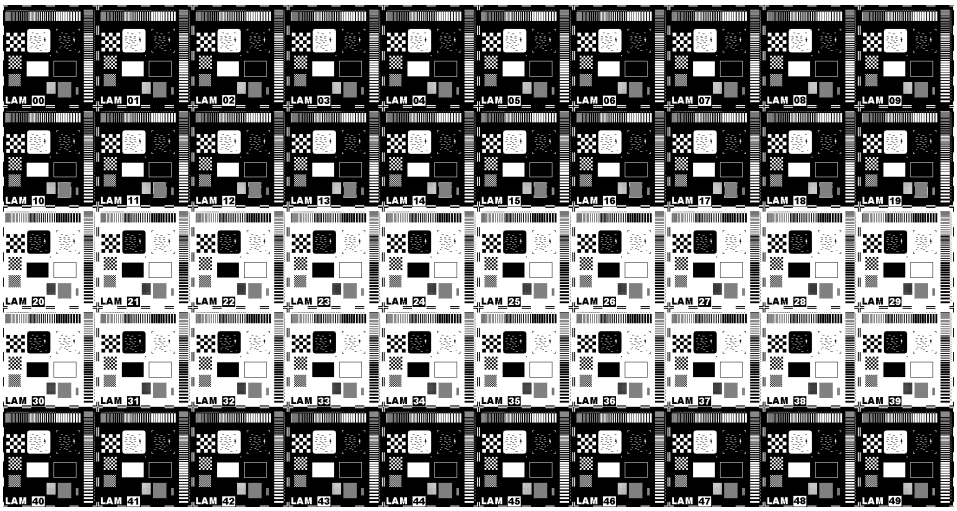

Figure 6*: LAM designed pattern (pattern 1).*

In order to optimize DMD testing, each DMD is tested with several patterns in parallel. For all optical tests the DMD micromirrors are divided into five individually managed pattern rows (Fig. 6): long exposure (EUCLID-type) or fast changing patterns (display-like), see also paragraph 3. The two major patterns, pattern 1 and pattern 2, are designed as "positive" and "negative" to each other (Fig. 6). Each pattern row is divided in 10 zones for a total of 50 zones, and each zone is imaged on the CCD camera (left-hand side of Fig. 7). Each zone includes specific patterns identical from zone to zone and numbers at the edge of each zone are set for easy processing and archiving (left-hand side of Fig. 7). The individual patterns show lines with different width and orientation, chessboard features and MOS-like patterns. In addition to pattern 1 and pattern 2, all ON and all OFF mirrors will also be displayed and measured at each measurement step. Background will be measured and subtracted from the images.

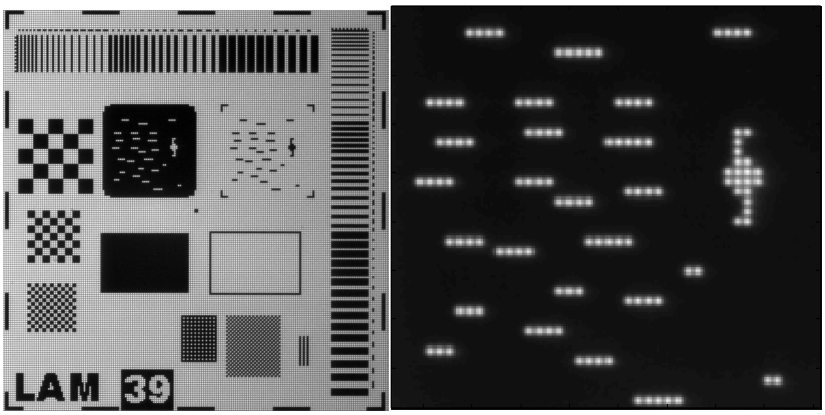

Figure 7: Image of a zone taken with the characterization set-up CCD camera and close-up view on a MOS-like pattern

Each micromirror is imaged on the CCD camera on about 4x4 detector pixels, which is enough for monitoring during the tests and detection of failures, if any. A zoom on the area simulating a MOS-like pattern, with multi-slits is shown in

right-hand side of Fig. 7. Any slit location and shape can be generated. It has to be noticed that the OFF mirrors cannot be imaged on the detector due to the high contrast performance of DMD. Then, the contrast cannot be measured in this test. An evaluation of the contrast will be done during the MOS-like tests, using a high dynamical range camera.

3.4 Analysis procedure

Data pipeline for data reduction has also been developed with Matlab software. Photometric measurements are done before, during and after each test, and compared to the reference measurements (before the test, at room temperature).

Any degradation in performance of a mirror will be revealed. Differences between mirrors as well as tests on different patterns applied on the same device (patterns in space domain and time domain) will be analyzed. The analysis procedure comprises background subtraction, patterns recentering, mirrors detection, comparison with the nominal mirror photometric measurement; local variations of the illumination beam are taken into account. Three mirror failure types exist: stuck or affected ON, stuck or affected OFF and stuck or affected during pattern switching. All failure types are searched and detected with the LAM software. Results are presented in the following sections.

4. RADIATION TESTING

Two DMD chip sets went through a preliminary Total Ionizing Dose (TID) radiation testing and provided a rough idea on how and at what radiation dose rate the DMD chip set would fail. Two additional DMD chip sets went through a second round of TID testing, which provided results with better details. The two TID test showed similar results so only the test setup and results of the second TID radiation campaign is presented here.

4.1 TID test setup

A complete test vehicle had to be in operation during the radiation testing, but by careful shielding with lead bricks, only devices under test received a significant radiation dose. The devices to be irradiated were selected in such a way that the artifacts of a failing device would help in pinpointing which device had failed. The devices to be irradiated were the DMD, one DDP1000, one RAMBUS memory and one DAD1000.

During the radiation testing the DMD displayed full black and full white test patterns that alternated every 1500 seconds. This is similar to the expected EUCLID duty cycle. A data logger measured the current consumption of major power supplies of the DMD chip set during radiation and provided the opportunity to monitor if and when any of the devices were degrading. Corresponding manual current measurements were done using a multimeter in between radiation steps and this provided better accuracy for understanding when and how the chips were failing. Visual inspection was done in between radiation steps by using an optical test set up that projected the center of the DMD on a projection screen and by visual inspection directly on the DMD. Both test vehicles went through 7 days of annealing at room temperature after completion of the irradiation sequence, cycling through the same set of test images as had been used in the radiation testing.

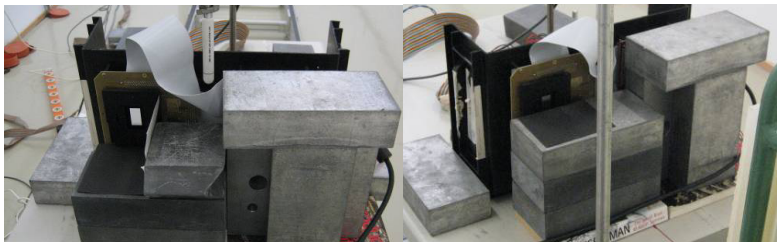

Figure 8: Pictures of the test set up of test 1 and test 2.

Two important differences in the TID testing between test 1 and 2 were

Smaller radiation dose: Test 1 received a radiation dose of 20 Krads, at which level the test vehicle started behaving incorrectly and were beyond any possible detailed optical characterization. Test 2 was therefore performed in smaller steps and aborted at a total dose level of 16 Krads, when the chip set started to have only minor artifacts, and could still go through a complete optical characterization.

Half of the DMD where shielded in test 2: Horizontal stripes related to the reset zones were apparent on the DMD in test 1. It was impossible to conclude if the stripes were caused by a degrading DMD, a degrading DAD1000 or a combination of the two. Test 2 was therefore conducted with half of the DMD shielded in order to see if the stripes became visible and if the stripes covered the irradiated half or both halves of the DMD.

4.2 TID test results

The manual current measurement from test 1 and 2 showed significant increases in current consumption on three power supplies during radiation and significant reduction in current consumption during annealing, see the table below.

TID	VCC2		12V		3V3		Visual observations
	Black	White	Black	White	Black	White	
Test 1 radiation testing, intermedia data							
0	0	0	42	42	132	133	-
2200	1	1	43	43	131	132	-
5000	0	0	42	42	134	134	-
10300	4	4	47	46	179	169	Faint stripes, related to reset lines
15300	47	45	91	89	816	486	Faint stripes, related to reset lines
20300	67	67	112	111	2109	836	Faint stripes, related to reset lines
Test 1 anneahiling, measurrement at start, stop and every day							
20300	50	49	95	93	348	176	Faint stripes, related to reset lines
20300	49	49	93	93	292	168	Faint stripes, related to reset lines
20300	46	45	90	89	242	159	Faint stripes, related to reset lines
20300	43	43	88	87	215	153	Very faint stripes, related to reset lines
20300	41	41	85	85	199	150	No stripes visible
20300	35	35	79	79	171	144	Hardly stripes, related to reset lines

TID	VCC2		12V		3V3		Visual observations
	Black	White	Black	White	Black	White	
Test 2 intermedia data							
0	0	0	41	40	133	134	-
10784	0	0	41	41	134	138	Very faint stripes, related to reset lines
10000	1	1	44	44	143	150	Faint stripes, related to reset lines
12200	6	6	49	49	179	193	Faint stripes, related to reset lines
14000	12	12	55	55	286	242	Faint stripes, related to reset lines
16000	23	23	66	65	464	349	Faint stripes, related to reset lines
Test 2 anneahiling data							
16000	7	7	48	48	152	149	Faint stripes, related to reset lines
16000	7	7	48	48	147	145	Faint stripes, related to reset lines
16000	6	7	48	48	147	144	Faint stripes, related to reset lines
16000	6	6	47	47	141	141	Faint stripes, related to reset lines
16000	6	6	47	47	139	139	Faint stripes, related to reset lines
16000	5	5	46	47	139	139	Faint stripes, related to reset lines

Table 1. TID test results for test 1 and 2 using flat black and flat white test patterns. VCC2 and 3V3 are power supplies for the DMD. 12V is the input power supply for the left DAD1000. Values in the VCC2, 12V and 3V3 columns are in mA.

The other power supplies remained stable during testing and data from these are not presented here. The data logger current measurements show a similar behavior as the manual measurement, but the results were noisy and are not presented here.

4.3 TID test results discussions

The sharp increase in current consumption on VCC2 and 3V3 power supplies from about 10 000 Krads are strong indications of a degrading DMD, see table 1. VCC2 is derived from the 12V input of the DAD1000 by an internal linear regulator, so an increase in current on the VCC2 results in the same increase in current on the 12V input. As can be seen in the table, this corresponds very well, and is a further indication of an affected DMD. Each DMD micromirror is backed by a SRAM memory cell. Since the voltage levels on the VCC2 and 3V3 are representative of the SRAM voltage levels, it is reasonable to suspect that it is the SRAM cells of each micromirror which is affected by radiation. The logic supporting the SRAM memory cells might be degrading as well, but any increase of current in this area will be swamped by the increase in the current consumption caused by the massive number of SRAM memory cells. A noteworthy result can be found by comparing the difference between test 1 and 2. Test 1 shows about double the current increase of test 2. This corresponds very well to the fact that in test 1, the whole DMD was irradiated while in test 2 only about half of the DMD was irradiated and about half was shielded. The current increase in test 2 is the result of the degradation caused by the half of the DMD that was not shielded.

At 20 Krads, the device from test 1 was degrading badly as visible in the picture below. Testing of device 2 was stopped at 16 Krads and had only minor artifacts that were not possible to capture on a digital camera under the test conditions. However, current measurements done during the annealing period showed a falling trend and tests conducted after the end of the annealing period showed normal operation on the DMD from test 1-2, suggesting full recovery of the DMDs.

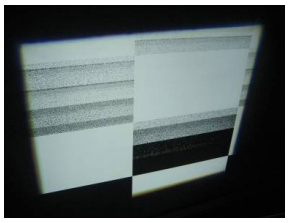

Figure 9: Corrupted DMD from test 1 at 20 Krads, displaying a flat white test picture.

4.4 TID test conclusion

The manual current measurements, the data logger current measurements and the visual observations show that the DMD starts to get affected at a dose rate of approximately 10 Krads, and will work with only minor artifacts up to a dose rate of about 16 Krads. Annealing of the DMD at room temperature in a biased condition brings the DMD back to normal operation again. The DDP1000, DAD1000 and the RAMBUS memory does not seem to be affected by these radiation levels.

5. COLD TEMPERATURE TEST

Two sets of cold temperature tests have been completed: the first test was done on a first device with the goal to reach a temperature level where the DMD could show major failures. A second test was done, cycling between a nominal temperature level (-40°C) and room temperature. This cycling was repeated three times during the test.

5.1 Cold temperature step stress test

The cold temperature step stress test has been done from room temperature down to -60°C; twelve temperature steps have been applied +20°C, +10°C, 0°C, -10°C, -20°C, -30°C, -35°C, -40°C, -45°C, -50°C, -55°C and -60°C. The test procedure is described in paragraph 3: the device was divided into 5 pattern rows and 50 zones. Within the 5 pattern rows, 4 were static pattern rows (EUCLID-type) and one was a switching pattern row (display type). The static pattern was frozen for 1500s. An optical measurement was then done with four consecutive applied patterns: pattern 1, pattern 2 (negative of pattern 1), all ON, all OFF and finally, the background (straylight in the environment when the input beam is blocked) was measured. All mirror failure types were then searched in stuck or affected ON, stuck or affected OFF and stuck or affected during pattern switching.

A section of the testing area is displayed in Fig. 10 for device temperature of -41°, -50°, -55°, -60°, and back to room temperature, at +24°. It is clear that one of the micromirrors that had been programmed to stay in an OFF position is blocked in an ON position during a pattern change (stuck mirror). This failure only occurred when a temperature of -55°C was reached. The degradation was apparent over the whole device, and was even worse when going to -60°C. **This test show that permanent failure is appearing on some mirrors when the device is taken down -55°C. The failure rate increases at -60°C.**

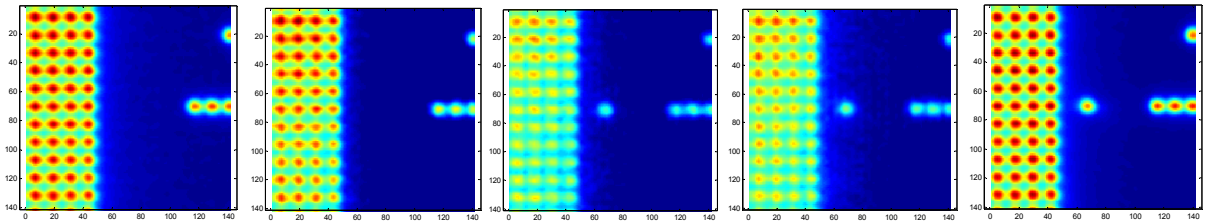

Figure 10: DMD detail image when the device temperature is at -41°, -50°, -55°, -60°, and back to room temperature +24°. A stuck mirror in ON position is revealed.

5.2 Nominal cold temperature test

Based on the results from the previous test, the nominal temperature condition for EUCLID was set at -40°C. In order to confirm that this is an acceptable nominal operating condition for the device, a DMD was mounted in the cold temperature chamber and tested three times at this temperature. For minimizing stress on the device when cooling down, a fast (-40°C / hour) and homogeneous cooling was provided thanks to numerous thermal links attached to the cooling system interface on one side and to the front plate as well as the heat sink of the DMD on the other side. Four measurements were done after three cycles running from room temperature to cold (-40°C) temperature and back to room temperature. These measurements have been done at +20°C, -38°C, -40°C, and -40°C.

We have adopted two mirrors failure definitions: - the **lossy mirror** when the throughput of the mirror is decreased by more than 30%.(this definition doesn't mean that the mirror is stuck). – the **weak mirror** when a loss in throughput between 10% and 30% is measured, with respect to their neighbour mirrors. By refining our data processing procedure, we are now able to detect any of these affected mirror behaviours (examples of lossy / weak mirrors given in Fig. 11).

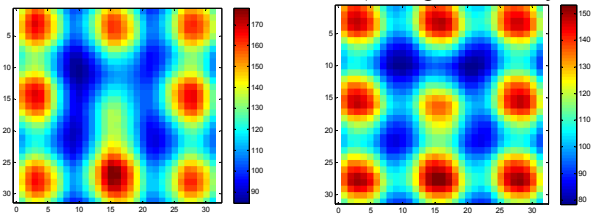

Figure 11:Lossy and weak mirrors (central mirror on the pictures).

Using the definitions of lossy and weak mirrors, we have analyzed all (over 2 million) mirrors from the DMD for each measurement. Results are displayed in a matrix format with the mirrors showing a failure displayed and numbered by zones (Fig. 12, 13 and 14). Measurements done at +20°C, -38°C, -40°C, and again -40°C resulted in total numbers of [lossy micromirrors + weak micromirrors] of 19 mirrors, 22 mirrors, 18 mirrors and 18 mirrors respectively. This shows that no degradation of the device is revealed when three consecutive cycles in EUCLID conditions are applied.

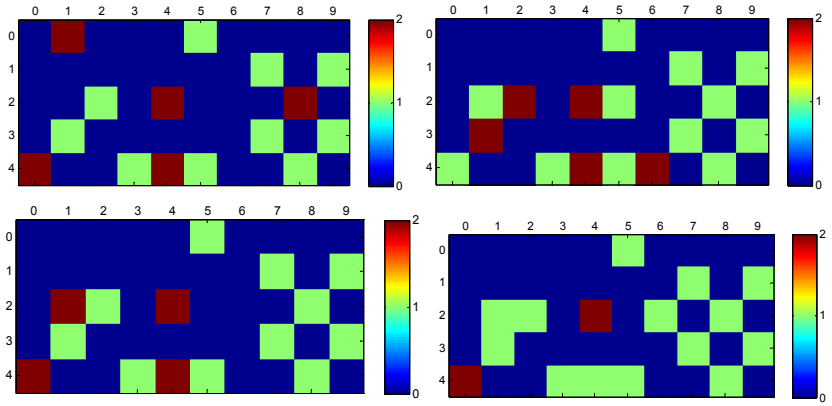

Figure 12: Location and numbers of mirror with any alteration (lossy and weak mirrors)
for measurements at +20°C, -38°C, -40°C, and again -40°C (from left to right and top to bottom)

If we enter in the details of the mirrors with important failures, i.e.lossy mirrors, they are all in the same location as the reference measurement at +20°C and all measurements around -40°C; this represents **12 mirrors** (Fig. 13). According to the screening procedure of TI where all mirrors are considered to be working (according to the binary projection criteria), this measurement shows a type of intermediate situation where lossy mirrors are observed, and they stay lossy during the whole test; all other mirrors show their full performances. This effect is possibly due to some local non-uniformity at individual mirror level, present since device fabrication. We highlight the fact that if this effect has no impact in usual DMD display mode, this effect has to be taken into consideration and calibrated for MOS application. Then, if the lossy mirrors are disregarded, the comparison of affected mirrors between ambient and cold temperature is only limited to the weak mirrors: for +20°C / -38°C: **7 mirrors;** for +20°C / -40°C: **4 mirrors; for** +20°C / -40°C: **3 mirrors.** This number is very low when compared to the total 2 millions mirrors operating in the device.

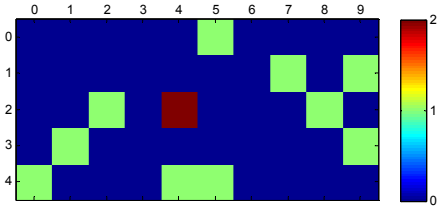

Figure 13: Location and numbers of mirror with only lossy mirrors for measurements at +20°C and -40°C

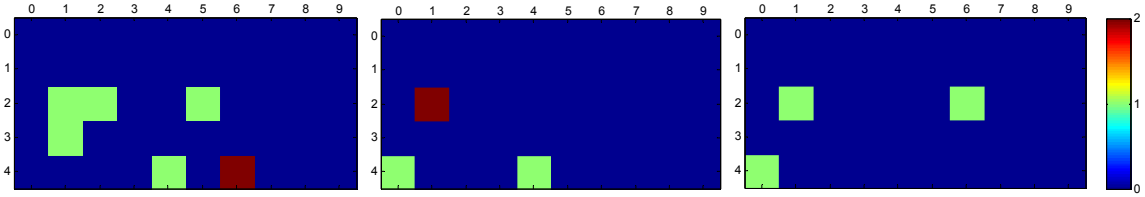

Figure 14: Comparison of affected mirrors between ambient and cold temperature (only weak mirrors):
+20°C / -38°C : **7 mirrors;** +20°C / -40°C : **4 mirrors;** +20°C / -40°C : **3 mirrors**

In conclusion, the micromirrors are operating properly at -40°C, and the differential failure rate between ambient and cold temperature, in EUCLID mode, is as low as: **3 to 7 mirrors over 2 million mirrors**. No stuck mirror has been observed, and for the lossy mirrors, if they are lossy at ambient, they stay lossy at cold temperature; mirrors affected afterwards are only failing as weak mirrors. From these charts, we clearly see the same behavior for mirrors switching frequently (display mode in the central pattern row) or in a static pattern during 1500s (EUCLID mission conditions), in the four other pattern rows.

6. LIFE TEST

The life test has been completed on one DMD device. The device was tested in EUCLID conditions, this means in vacuum, at -40°C and the device was operating with the following test cycle: pattern 1 is applied during 1500s (central pattern row is tilting in display mode while others pattern rows stay with static pattern), switching of the whole device between pattern 1 and pattern 2 during 60s, pattern 2 is applied during 1500s (central pattern row is tilting in display mode while others pattern rows stay with static pattern). By this way, there is an identical duty cycle for all mirrors. **The life test lasted for 1038 hours.** Full optical tests were done during the whole life test. Measurements were done at room temperature (reference measurement), a first test at cold temperature was done at T0, then 11 intermediate measurements were done, and finally, a last measurement was done at the end of the life test, after **1038h.**

During the whole test, DMD operational temperatures were recorded:

- DMD heat sink temperature (closed to the actual DMD component temperature point): **-41°C**
- DMD front mounting surface temperature: **-36°C**
- Thermal interface temperature: **-49°C**

We can note that when the DMD is stopped, a drop of **2-3°C** in temperature is revealed, showing the heating capability of the DMD chip due to its power consumption.

A picture of the device during the life test is shown in Fig. 15. A preliminary analysis has been done only on the central pattern row (10 zones). Location and number of mirrors with any failure (lossy and weak micromirrors) for measurements at +20°C are shown in Fig. 15. The number is low: 11 mirrors.

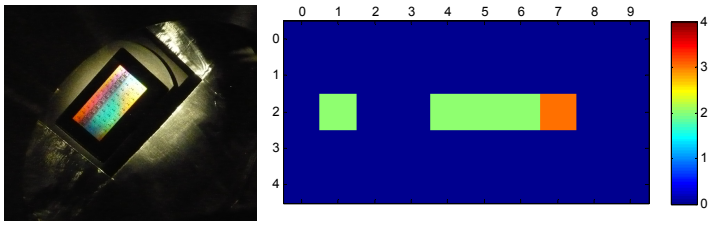

Figure 15: Picture of the device during the life test.
Location and number of mirrors with any failure for measurements at +20°C.

Location and number of affected mirrors (lossy and weak micromirrors) for measurements at -41°C at 0h of the life test and at 802h of the life test are shown in Fig. 16. The numbers are also low: 16 and 23 mirrors respectively.

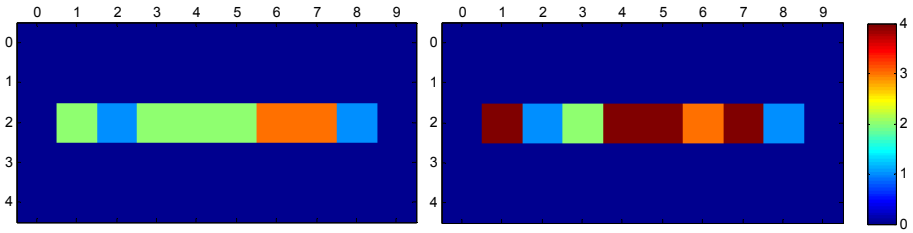

Figure 16: Location and number of mirrors with any failure for measurements at -41°C at 0h and at 802h of the life test

Full analysis of this life test (on the total DMD surface) is under way. Life test measurements will be completely analyzed, and we will investigate the DMD behavior revealed by this test. This first life test has been successfully completed on the DMD device.

7. CONCLUSION

The EUCLID mission from the European Space Agency (ESA) will study the dark universe; a multi-object spectrograph (MOS) option is under study. These arrays will act as reconfigurable objects selection masks. ESA has engaged with Visitech and LAM for a technical assessment of the DMD chip from Texas Instruments, that features a 2048 x 1080 mirrors and a pixel pitch of 13.68µm, for space application. Specialized driving electronics and a cold temperature test set-up have been developed.

Cold temperature tests and 1038h life test have been completed successfully, following our test plan. TID radiation effects were observed with recovery after annealing. The results obtained up to now do not reveal any show-stopper concerning the ability of the DMD to meet environmental EUCLID requirements.

Thermal cycling and vibrations tests are due for March 2010, and full review of DMD performances will be conducted at the end of all tests.

From an ESA perspective, the micromirror arrays have therefore achieved a reasonable TRL (Technology Readiness Level). Insertion of such devices into final flight hardware would however still require additional time consuming (estimation is approximately 2 years) efforts in terms of replacement of the window coating, re-development of space compatible electronics as well as a different package interface compatible with spacecraft launch conditions. These additional developments are expected to be addressed in a possible follow-on activity.

ACKNOWLEDGEMENT

The authors thank Jean-Antoine Benedetti, Philippe Laurent and Vincent Herault from LAM for their assistance during the tests. This work is partly funded by ESA, CNRS, Provence-Alpes-Cote d'Azur regional council and Conseil General des Bouches-du-Rhone county council.

REFERENCES

1. R. Burg, P.Y. Bely, B. Woodruff, J. MacKenty, M. Stiavelli, S. Casertano, C. McCreight and A. Hoffman, "Yardstick integrated science instrument module concept for NGST", in *Proceedings of the SPIE conference on Space Telescope and Instruments V*, SPIE **3356**, 98-105, Kona, Hawaii, 1998
2. F. Zamkotsian, K. Dohlen, D. Burgarella, V. Buat, "Aspects of MMA for MOS: optical modeling and surface characterization, spectrograph optical design", in *Proceedings of the NASA conference on "NGST Science and Technology Exposition"*, ASP Conf. Ser. **207**, 218-224, Hyannis, USA, 1999
3. M. Robberto, A. Cimatti, A. Jacobsen, F. Zamkotsian, F. M. Zerbi, "Applications of DMDs for Astrophysical Research", in *Proceedings of the SPIE conference on MOEMS 2009*, Proc. SPIE **7210**, San Jose, USA (2009)
4. H. Moseley, S. Aslam, M. Baylor, K. Blumenstock, R. Boucarut, A. Erwin, R. Fettig, D. Franz, T. Hadjimichael, J. Hein, A. Kutyrev, M. Li, D. Mott, C. Monroy, D. Schwinger "Microshutter arrays for the NGST NIRSpec", in *Proceedings of the SPIE conference on Astronomical Telescopes and Instrumentation 2002*, Proc. SPIE **4850**, Hawaii, USA, 2002
5. S. Waldis, F. Zamkotsian, P. Lanzoni, W. Noell, N. de Rooij, "Micromirrors for multiobject spectroscopy: optical and cryogenic characterization", in *Proceedings of the SPIE conference on MOEMS 2008*, Proc. SPIE **6887**, San Jose, USA (2008)
6. F. Zamkotsian, K. Dohlen, "Performance modeling of JWST Near Infrared Multi-Object Spectrograph," in *Proceedings of the SPIE conference on Astronomical Telescopes and Instrumentation 2004*, Proc. SPIE **5487**, Glasgow, United Kingdom (2004)
7. F. Zamkotsian, J. Gautier, P. Lanzoni, "Characterization of MOEMS devices for the instrumentation of Next Generation Space Telescope," in *Proceedings of the SPIE conference on MOEMS 2003*, Proc. SPIE **4980**, San Jose, USA (2003)
8. F. Zamkotsian and K. Dohlen, "Surface characterization of micro-optical components by Foucault's knife-edge method: the case of a micro-mirror array", Applied Optics, **38** (31), 6532-6539 (1999)
9. A. Liotard, F. Zamkotsian, "Static and dynamic micro-deformable mirror characterization by phase-shifting and time-averaged interferometry", in *Proceedings of the SPIE conference on Astronomical Telescopes and Instrumentation 2004*, Proc. SPIE **5494**, Glasgow, United Kingdom (2004)